

Computational simulations of blown sand flux over complex microtopography

Huang Ning and Shi Feng

*Key Laboratory of Mechanics on Western Disaster and Environment,
Lanzhou University, Lanzhou, China
Email: huangn@lzu.edu.cn*

Abstract: Current research on sand saltation concentrates on wind tunnel experiment, theoretical analysis and numerical simulation of sand saltation at ideal and controllable conditions, for example, time-invariant wind speed and flat sand bed. However, these somehow idealized theoretical analyses and numerical simulations can not accurately predict sand movements in field environments, which are generally composed of surface obstacles including dunes and bushes.

In this paper, the simulation object is merely a barchan dune (38°47'22"N and 102°29'25"E) nearby the meteorology tower of Integrated Desert Control Experimental Station in Minqin area. Minqin is a county of Gansu province of China, which locates between edges of the Badain Jaran Desert and the Tengger Desert. The tri-dimensional and unstructured grid system was generated with the grid generator GAMBIT. The model of the barchan dune is within 1.1×10^6 tetrahedral cells and 2.3×10^5 nodes, and its domain is 360×280×60m (length, width, height). The shear-stress transport (SST) $k-\omega$ turbulence model available in FLUENT software 6.3 version was employed. The eight cup anemometers and six long-averaging-time collectors (BSNE stood for Big Spring Number Eight) used to measure wind speed and sand mass flux. It is found that simulated wind speed and sand flux agrees with the measurement data. Meanwhile, the sand flux increases from the right horn of the dune, gets the maximum at the intersection point of the dune longitudinal section and brink, and decreases to the left horn of the dune.

Keywords: *computational simulation, friction velocity, sand transport, wind field modeling, sand flux*

1. INTRODUCTION

Current research on sand saltation concentrates on wind tunnel experiment, theoretical analysis and numerical simulation of sand saltation at ideal and controllable conditions, for example, time-invariant wind speed and flat sand bed (Bauer *et al.*, 1998; Huang *et al.*, 2007; Leenders *et al.*, 2005; Shao, 2008; van Boxel *et al.*, 1999; Zheng *et al.*, 2004; Zheng *et al.*, 2003; Zheng *et al.*, 2006b; Zhou *et al.*, 2002; Zou *et al.*, 2001). Recently, the 6th International Conference on Aeolian Geomorphology (ICAR VI) was held from July 23–28, 2006 at the University of Guelph (Ontario, Canada), many achievements were made in the physics of wind-blown sand (Bauer, 2009; Lancaster, 2008), e.g. Zheng and co-workers established the stochastic particle-bed collision model to obtain the lift-off velocity distribution function of sand particles (Zheng *et al.*, 2006b), and were the first to account for the effects of electrostatic forces (Yue and Zheng, 2006; Zheng *et al.*, 2006a; Zheng *et al.*, 2003). Zheng *et al.*, (2009) proposed a scale-coupled method for the formation and evolution of aeolian sand dune fields, which successfully reproduces various dune patterns and the whole development process of a dune field of several square kilometers during several decades. These remarkable achievements have profoundly revealed the underlying dynamic mechanism of wind-blown sand movement.

However the present theoretical analysis and numerical simulation of sand movement are far from accurately predicting sand movement in the field environment, which is generally composed by surface obstacles, for example dune and bush. Therefore research on wind field and sand saltation flux in complex microtopography is significant and more scientists have conducted field measurements to study characteristics of blown sand flux in these environments (Bauer *et al.*, 1998; Bowker *et al.*, 2007; Leenders *et al.*, 1998; van Boxel *et al.*, 2004). Sand fluxes at some locations over the barchan dune in Minqin have been calculated based on the simulated wind field in this paper.

2. MEASUREMENT AND SIMULATION OF WIND SPEED AND SAND FLUX

2.1. Simulation objects

The simulation object is merely a barchan dune nearby the meteorology tower of Integrated Desert Control Experimental Station in Minqin area. Minqin is a county of Gansu province of China, which locates between edges of the Badain Jaran Desert and the Tengger Desert. The morphology of a barchan is as illustrated in Figure 1, which (38°38'00"N and 102°55'12"E) is approximately 14.28m in height, 159.40m in width between two horns, with 81.26m long and 10.12° of the windward slope, 22.61m long and 30.27° of the leeward slope, and 20.03° between the longitudinal centerline of the dune and the East direction. The six white diamonds express the sand flux spots, the two black diamonds are the wind speed measuring spots. There are six long-averaging-time collectors (BSNE) of horizontal mass flux (Fryrear, 1986), which has an overall sampling efficiency between 86% and 95% for sand flux measurement (Shao *et al.*, 1993), a vane and four lightweight fast-responding cup anemometers, which were voltage-generating units (R. M. Young Model 03001) with a threshold speed of about 0.5 ms⁻¹, mounted at a straight and metallic bar along the gravity direction and sampled at a frequency of 1 Hz. The data was synchronously recorded by a Campbell Scientific CR 3000 Datalogger. At spot A, four anemometers are 0.08, 0.43, 0.93 and 1.92m above the dune surface. At spot B four anemometers are 0.12, 0.45, 0.89 and 1.92m from the dune surface. The 0° value of vane means the North. The inflow direction of this sand storm is northwest, namely inflow direction is from 280°-340°.

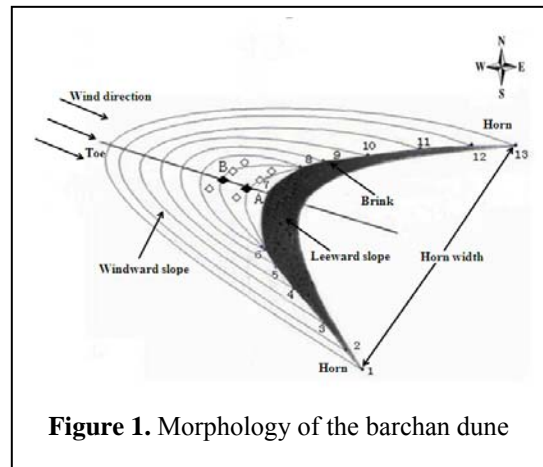


Figure 1. Morphology of the barchan dune

A fully turbulent atmospheric boundary layer over a flat surface shows a logarithmic increase of the velocity $U(z)$ with the distance z from the surface. Therefore, a logarithmic velocity profile on the inlet of the form:

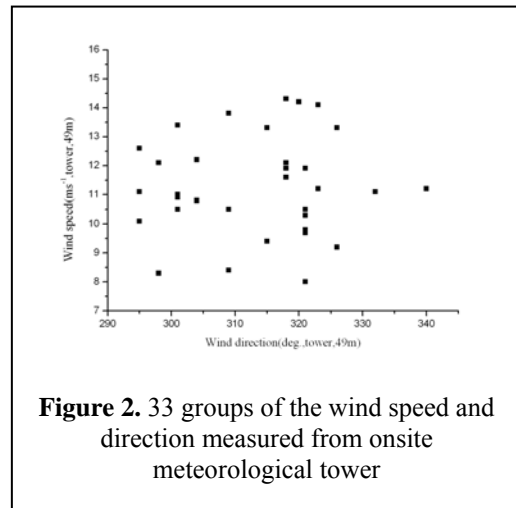
$$U(z) = \frac{u_*}{\kappa} \ln\left(\frac{z}{z_0}\right) \quad (1)$$

Where z_0 is the aerodynamic roughness length of the surface and $\kappa=0.4$ is the von Karman coefficient (Shao, 2008). u_* is the friction velocity and is defined by the value of reference velocity, U_{ref} was taken at the topmost measurement point of the meteorological tower because the value is, presumably, the least affected

by the lower level flow disturbances resulting from wind interactions with the dune. While the direction of reference velocity, U_{ref} also defined the inflow direction. The reference velocities were taken 33 groups of the wind speed and direction at the height of 49m which is the topmost measurement point of the meteorological tower near the barchan dune in Figure 2. Other results of sand flux, wind speed and direction on the windward slope of the dune were measured in a 5.5 hours sand storm (14:00-19:30) March 17, 2008.

2.2. Methodology

The vertical distribution of the inflow velocity follows the logarithmic law of a fully developed boundary layer by Eq. (1). At the outlet profile, the flow was assumed as a fully-developed flow, the outflow boundary condition was applied, and, thus, the conditions of the outlet plane were extrapolated from within the domain and had no impact on the upstream. As the top boundary was placed far enough outside the boundary layer, symmetry boundary conditions were applied to enforce a parallel flow by forcing the velocity component normal to the boundary to vanish and prescribing zero normal derivatives for all other flow variables, and the non-slip boundary conditions were applied on the surface. In this study, the tri-dimensional and unstructured grid system was generated with the grid generator GAMBIT. The barchan dune is within 1.1×10^6 tetrahedral cells and 2.3×10^5 nodes, and its domain is $360 \times 280 \times 60$ m (length, width, height). Because the geometry shape of microtopography is complex, the shear-stress transport (SST) $k-\omega$ turbulence model available in FLUENT software 6.3 version was employed for the modelling of the flow and turbulence within the Minqin dune. This model was developed to effectively blend the robust and accurate formulation of the $k-\omega$ model in the near-wall region with the free-stream independence of the $k-\epsilon$ model in the far field (FLUENT, 2006).



3. RESULTS AND DISCUSSIONS

3.1. Wind field over a dune in Minqin

Figure 3(a) and Figure 3(b) present some of the major streamlines around the barchan dune and streamwise velocity field of vertical section and transverse section of the dune under 321° wind direction. The vertical section is through dune apex and parallel to wind flow direction. The transverse section is 10m above the ground level. Figure 3(a) shows the flow separation at the top of the dune and a large eddy that forms in the wake of the dune. The result is consistent with published field data of wind flow over dunes (Neuman *et al.*, 2000; Walker and Nickling, 2002; Wiggs *et al.*, 1996). Figure 3(b) shows that there are two unsymmetrical vortices in the wake of the dune, which are affected by the shape of the dune, inflow wind speed and direction.

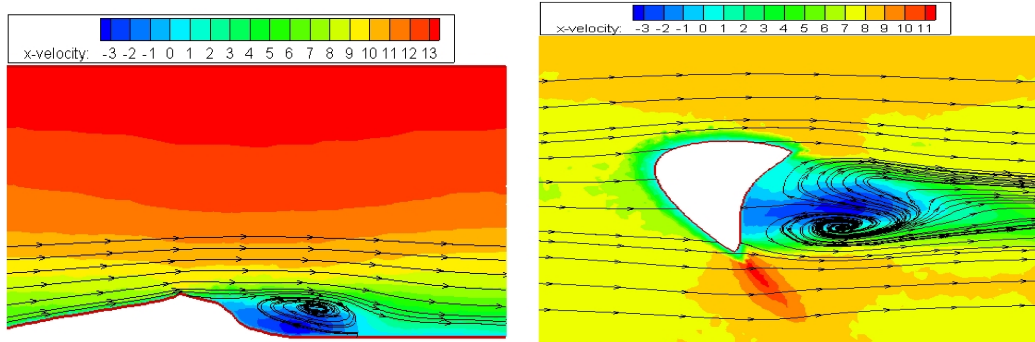


Figure 3(a) Vertical section

Figure 3(b) Transverse section

Figure 3 Streamwise velocity field over the barchan dune

Figure 4 shows the comparison between the simulated and measured results of wind speed above 1.92m dune surface at spot A and B under 33 inflow conditions. The accuracy of error in the prediction of the measured values is mostly within $\pm 2.5 \text{ms}^{-1}$, and the correlation coefficient between simulated results and measured results of wind speed is 0.5652 and 0.6552 respectively.

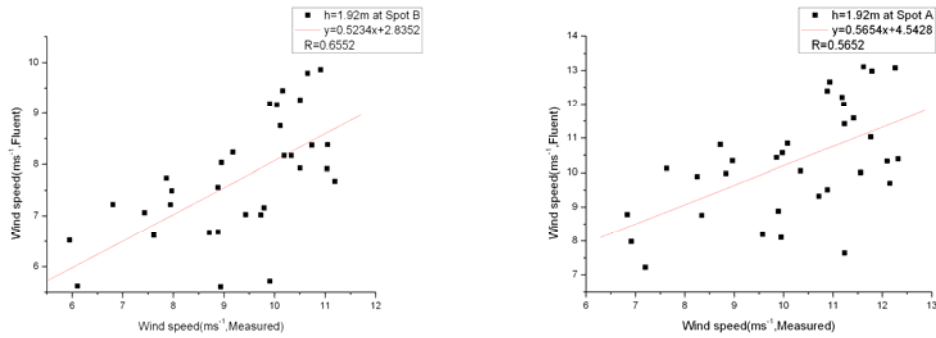


Figure 4 Comparison between the simulated and measured results of wind speed at spot A and B

3.2. Sand flux over a dune in Minqin

In order to calculate sand flux, Owen(1964) model is applied in this paper:

$$G = c_0 \rho / g u_*^3 \left(1 - u_{*t}^2 / u_*^2 \right) \quad (2)$$

where G is sand flux, c_0 is a empirical coefficient, $\rho=1.225\text{kgm}^{-3}$ is the air density, g is the acceleration of gravity, u_* and u_{*t} are the friction velocity and threshold friction velocity respectively. For the sand flux simulations, we assume that wind velocity obeys logarithmic velocity gradient, the roughness length for that gradient does not vary between locations, and a threshold velocity where sand first begins to move can be found on the basis of threshold friction velocity. So the Eq. (2) can be changed to Eq. (3):

$$G = A_1 u^3 \left(1 - u_t^2 / u^2 \right) \quad (3)$$

Where A_1 is experimental coefficient, u and u_t are the wind speed and threshold wind speed above 0.6m dune surface respectively. Before calculate sand flux, we need to get A_1 and u_t , which are related to the local surface conditions and can be determined by fitting the measurement results of BSNE collectors with the total simulated time-integrated fluxes at six sediment collectors' locations to Eq. (3). That is, calculate the sand fluxes with Eq. (3) with the wind speed and threshold wind speed above 0.6m dune surface at six measured points and integrate the fluxes over time to get the total sand fluxes (including the variables A_1 and u_t). By comparing the calculated total sand fluxes with field measurement data, the optimized values of the coefficient A_1 and the threshold wind speed u_t with which the calculated sand fluxes are most befitting with the corresponding data of measurement can be obtained. Using the above method proposed by Bowker *et al.* (2007), we find that the coefficient $A_1=2.158 \times 10^{-5} \text{kgs}^2\text{m}^{-4}$ and the threshold wind speed is $u_t=5.1\text{m s}^{-1}$.

Figure 5 presents a comparison at six spots between the simulated total sand fluxes and corresponding measurements for a 5.5 hours sand storm (17 March 2008). From Figure 7 it can be seen that 5 out of 6 differences between the simulated results and measurements are smaller than 10%, and the correlation coefficient is 0.6337, so that it is applicable to simulate sand flux over complex microtopography in this paper.

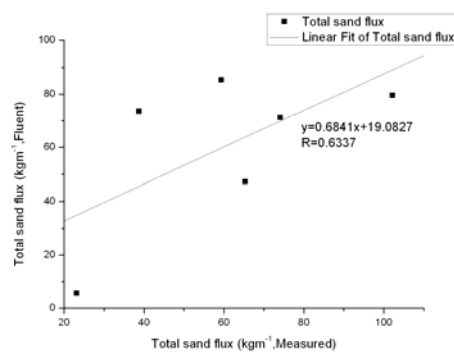


Figure 5 Comparison between the simulated total sand fluxes and corresponding measurements at six spots

Figure 6 shows the simulated sand fluxes at thirteen positions of the dune brink under 298° and 321° wind directions. The thirteen positions are illustrated by nodes on the dune brink from left to right in turn in Figure 2. Figure 6 shows that the sand flux increases from the right horn of the dune, gets the maximum at the intersection of the brink and the longitudinal centerline of the dune, and then decreases to the left horn of the dune. It suggests sand, by saltation and surface creep, upwards across the gentle windward slope, arrives at the brink of barchans dune, and is deposited by avalanche on the lee slope (Bagnold, 1941). Because the different angle between

dune transverse section and wind direction, the sand fluxes under 321° of wind direction are bigger than that under 298° of wind direction. But the simulated sand flux shows the same variation trend along the dune brink under both wind directions, while this is the reason that the right horn area of the dune is more than the left horn area.

4. CONCLUSIONS

The wind flow over a barchan dune in Minqin under 33 kinds of flow boundary condition is simulated. Based on the simulated wind flow, the sand fluxes at six spots on the dune are calculated by Owen (1964) model. The calculated results have been compared with the measured sand fluxes. Several conclusions can be summarized as follows:

- through comparing the simulated sand flux with that of measurement at six measured spots, it is discovered that simulated sand flux agrees with the measurement data, which indicates that it is accurate to calculate the sand flux over natural complex microtopography by Owen model;
- the sand flux increases from the right horn of the dune, gets the maximum at the intersection point of the dune longitudinal section and brink, and decreases to the left horn of the dune.

ACKNOWLEDGMENTS

This research work was supported by a grant of the National Key Project for basic research(2009CB421304) and the Natural Science Foundation of China (Grant No. 10772073;10811130470), and the Science Fund of the Ministry of Education of China for PhD Program (Grant No. 20060730014). The authors sincerely appreciate this support.

REFERENCES

Bauer, B.O., (2009), Contemporary research in aeolian geomorphology. *Geomorphology*, 105(1-2): 1-5.

Bauer, B.O., Yi, J.C., Namikas, S.L. and Sherman, D.J., (1998), Event detection and conditional averaging in unsteady aeolian systems. *Journal of Arid Environments*, 39(3): 345-375.

Bowker, G.E., Gillette, D.A., Bergametti, G., Marticorena, B. and Heist, D.K., (2007), Sand flux Simulations at a small scale over a heterogeneous mesquite area of the northern chihuahuan desert. *Journal of Applied Meteorology and Climatology*, 46(9): 1410-1422.

FLUENT, (2006), FLUENT 6.3 User's Guide. *Fluent Inc.*

Huang, N., Zhang, Y.L. and D'Adamo, R., (2007), A model of the trajectories and midair collision probabilities of sand particles in a steady state saltation cloud. *Journal of Geophysical Research*, 112, D08206 doi:10.1029/2006JD007480

Lancaster, N., and B. Marticorena, (2008), Introduction to special section on Aeolian Processes: Field Observations and Modeling. *Journal of Geophysical Research-Earth Surface*, 113(F2).

Leenders, J.K., van Boxel, J.H. and Sterk, G., (2005), Wind forces and related saltation transport. *Geomorphology*, 71(3-4): 357-372.

Neuman, C.M., Lancaster, N. and Nickling, W.G., (2000), The effect of unsteady winds on sediment transport on the stoss slope of a transverse dune, Silver Peak, NV, USA. *Sedimentology*, 47(1): 211-226.

Owen, P.R., (1964), Saltation of uniform grains in air. *Journal of Fluid Mechanics*, 20(2): 225-242.

Shao, Y.P., (2008), Physics and Modelling of Wind Erosion. Springer, University of Cologne, Germany.

van Boxel, J.H., Arens, S.M. and Van Dijk, P.M., (1999), Aeolian processes across transverse dunes. I: Modelling the air flow. *Earth Surface Processes and Landforms*, 24(3): 255-270.

van Boxel, J.H., Sterk, G. and Arens, S.M., (2004), Sonic anemometers in aeolian sediment transport research. *Geomorphology*, 59(1-4): 131-147.

Walker, I.J. and Nickling, W.G., (2002), Dynamics of secondary airflow and sediment transport over and in the lee of transverse dunes. *Progress in Physical Geography*, 26(1): 47-75.

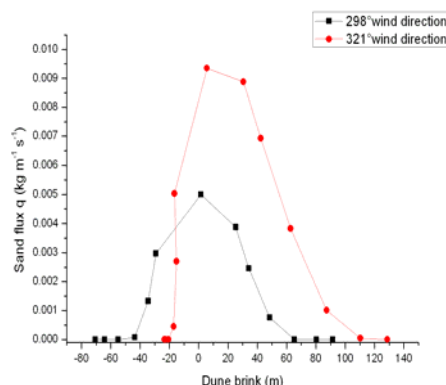


Figure 6 The simulated sand fluxes at thirteen positions of the dune brink under 298° and 321° wind directions

- Wiggs, G.F.S., Livingstone, I. and Warren, A., (1996), The role of streamline curvature in sand dune dynamics: Evidence from field and wind tunnel measurements. *Geomorphology*, 17(1-3): 29-46.
- Yue, G.W. and Zheng, X.J., (2006), Electric field in windblown sand flux with thermal diffusion. *Journal of Geophysical Research-Atmospheres*, 111, (D16) D16106, 10.1029/2005jd006972
- Zheng, X.J., Bo, T.L. and Zhu, W., (2009), Ascale-coupled method for simulation of the formation and evolution of aeolian dune field. *International Journal of Nonlinear Sciences & Numerical Simulation*, 10(3): 387-395.
- Zheng, X.J., He, L.H. and Wu, J.J., (2004), Vertical profiles of mass flux for windblown sand movement at steady state. *Journal of Geophysical Research*, 109, B01106 doi:10.1029/2003JB002656
- Zheng, X.J., Huang, N. and Zhou, Y., (2006a), The effect of electrostatic force on the evolution of sand saltation cloud. *European Physical Journal E*, 19(2): 129-138.
- Zheng, X.J., Huang, N. and Zhou, Y.H., (2003), Laboratory measurement of electrification of wind-blown sands and simulation of its effect on sand saltation movement. *Journal of Geophysical Research*, 108, (D10) 4322 doi:10.1029/2002JD002572
- Zheng, X.J., Xie, L. and Zou, X.Y., (2006b), Theoretical prediction of liftoff angular velocity distributions of sand particles in windblown sand flux. *Journal of Geophysical Research*, 111, D11109 doi:10.1029/2005JD006164
- Zhou, Y.H., Guo, X. and Zheng, X.J., (2002), Experimental measurement of wind-sand flux and sand transport for naturally mixed sands. *Physical Review E*, 66, doi:10.1103/PhysRevE.66.021305
- Zou, X.Y. et al., (2001), The distribution of velocity and energy of saltating sand grains in a wind tunnel. *Geomorphology*, 36(3-4): 155-165.